Bioorganic & Medicinal Chemistry Letters xxx (2016) xxx–xxx

Contents lists available at ScienceDirect

Bioorganic & Medicinal Chemistry Letters

journal homepage: www.elsevier.com/locate/bmcl

N-Arylsulfonyl-α-amino carboxamides are potent and selective inhibitors of the chemokine receptor CCR10 that show efficacy in the murine DNFB model of contact hypersensitivity

Asitha Abeywardane, Gary Caviness, Younggi Choi, Derek Cogan *, Amy Gao, Daniel Goldberg, Alexander Heim-Riether, Debra Jeanfavre, Elliott Klein, Jennifer A. Kowalski, Wang Mao, Craig Miller, Neil Moss, Philip Ramsden, Ernest Raymond, Donna Skow, Lana Smith-Keenan, Roger J. Snow, Frank Wu, Jiang-Ping Wu, Yang Yu

Boehringer Ingelheim Pharmaceuticals, Inc., 900 Ridgebury Road, Ridgefield, CT 06877, USA

ARTICLE INFO

Article history:
Received 29 June 2016
Revised 15 September 2016
Accepted 16 September 2016
Available online xxxx

Keywords:
CCR10
CCL27
Psoriasis
Contact hypersensitivity
Structural alerts

ABSTRACT

Compound **1** ((4-amino-3,5-dichlorophenyl)-1-(4-methylpiperidin-1-yl)-4-(2-nitroimidazol-1-yl)-1-oxobutane-2-sulfonamido) was discovered to be a 690 nM antagonist of human CCR10 Ca^{2+} flux. Optimization delivered (2*R*)-4-(2-cyanopyrrol-1-yl)-*S*-(1*H*-indol-4-yl)-1-(4-methylpiperidin-1-yl)-1-oxobutane-2-sulfonamido (**eut-22**) that is 300 fold more potent a CCR10 antagonist than **1** and eliminates potential toxicity, mutagenicity, and drug–drug-interaction liabilities often associated with nitroaryls and anilines. **eut-22** is highly selective over other GPCR's, including a number of other chemokine receptors. Finally, **eut-22** is efficacious in the murine DNFB model of contact hypersensitivity. The efficacy of this compound provides further evidence for the role of CCR10 in dermatological inflammatory conditions.

The control of T cell homing to different tissues during inflammation is the result of the interplay of selectins, integrins and chemokine receptors (CCRs), resulting in the direction of distinct T cell subsets to specific inflammatory sites[1,2] The chemokine receptor CCR10 plays an important role in the migration of skin-homing memory T-cells to the skin[3,4] through activation by the chemokine CCL27/CTACK or to mucosal epithelia through activation of CCL28.[5] Both CCR10 and CCL27 are associated with inflammatory skin diseases such as allergic contact dermatitis and psoriasis.[6–8] Notably, interruption of the CCL27–CCR10 interaction with anti-CCL27 antibodies suppresses allergen-induced skin inflammation.[6] These reports suggest disruption of the CCL27–CCR10 interaction may be a promising treatment for inflammatory skin diseases. However, the impact of blocking CCR10 directly on inflammation in the skin has not been reported. Indeed, there are contradictory reports of whether CCR10 antagonism is sufficient for a robust anti-inflammatory response, or whether intervention at other signaling pathways is also required.[9–12] We embarked on a program to discover and optimize selective small molecule antagonists of CCR10 and to elucidate the role of CCR10 in inflammatory skin diseases. Herein we describe the discovery and optimization of potent CCR10 antagonists that further demonstrate efficacy in a murine model of contact hypersensitivity.

We began by screening for inhibitors of the CCL27 dependent Ca^{2+} flux in CHO-K cells stably transfected with both human CCR10 and aequorin.[13] Our screen identified compound **1** with a CCR10 IC_{50} of 690 nM. Compound **1** (Fig. 1) also demonstrated further functional CCR10 antagonism by inhibiting the CCL27 dependent chemotaxis of Ba/F3 cells stably transfected with human CCR10 with an IC_{50} of 53 nM. However, 20 μM of **1** exhibited no

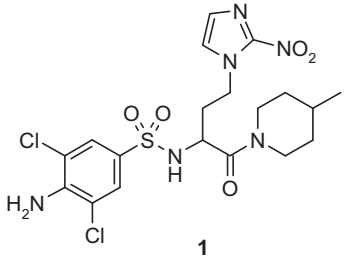

1

Figure 1.

* Corresponding author. Tel.: +1 203 791 6187.
E-mail address: derek.cogan@boehringer-ingelheim.com (D. Cogan).

http://dx.doi.org/10.1016/j.bmcl.2016.09.047
0960-894X/

antagonism of murine CCL27 dependent Ca^{2+} flux in CHO-K cells stably transfected with murine CCR10 despite 88% sequence identity (90% homology) between human and murine CCR10.

Compound **1** also contains at least two structural alerts associated with toxicity in the nitro group and the aniline.[14] We began optimization efforts by establishing SAR trends that could avoid the nitro and aniline. Meanwhile, we tracked our progress against the murine receptor to establish whether functional probes for murine models of skin inflammation would emerge.

The synthesis of compounds **1**–**38** are summarized in Schemes 1–3, and have been described elsewhere.[15] Bromide **39** was prepared from γ-aminobutyrolactone via the published procedure.[16] Imidazole, 2-nitroimidazole, 2-chloroimidazole, pyrazole, 1,2,3-triazole, 1,2,4-triazole, 2-cyanopyrrole, and pyrrole were alkylated with **39** to provide **40a**–**i**, with 1,2,3-triazole generating a separable mixture of **40e** and **40f** in a 2:1 ratio. The final products were prepared from *N*-Boc-amino acids **41a**–**o** via amide coupling with 4-methylpiperidine, followed by Boc removal, and treatment of the resulting amine with the appropriate sulfonyl chloride in the presence of an acid scavenger. The homophenylalanine compounds *R*-**10** and *S*-**10** were respectively prepared from commercially available (*R*)- and (*S*)-Boc-homophenylalanine. **41l**, **41m**, and **41n** were prepared via Strecker chemistry as described previously.[17]

The sulfonyl chlorides used to prepare **15**, **16**, **17**, **23**, and **24** were obtained from commercial vendors. 4-Amino-3,5-dichlorobenzene-sulfonyl chloride and 3-amino-2,4-dimethylbenzenesulfonyl chloride were prepared by chlorosulfonylation of 2,6-dichloroaniline and 2,6-dimethylanline respectively. The indolesulfonyl chlorides (**43a**–**f**) were prepared from the corresponding bromoindole via bromine-halogen exchange with *t*-butyllithium followed by quenching with saturated SO_2 in THF (Scheme 2). The resulting lithium sulfinate was then oxidized to the sulfonyl chloride with NCS. In some cases, the indole was protected as a Boc carbamate. In these cases, the final sulfonamide product was treated with HCl in dioxane to provide the product.

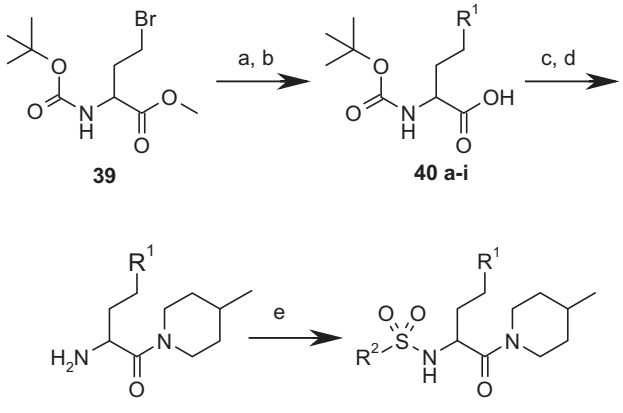

41 a R^1 = 2-nitroimidazol-1-yl
b R^1 = imidazol-1-yl
c R^1 = 2-cyanoimidazol-1-yl
d R^1 = 2-chloroimidazol-1-yl
e R^1 = 1,2,3-triazol-1-yl
f R^1 = 1,2,3-triazol-2-yl
g R^1 = 1,2,4-triazol-1-yl
h R^1 = pyrazol-1-yl
i R^1 = pyrrol-1-yl
j R^1 = R-phenyl
k R^1 = S-phenyl
l R^1 = 2-chlorophenyl
m R^1 = 5-cyanopyrazol-1-yl
n R^1 = 5-chloropyrazol-2-yl
o R^1 = 2-cyanopyrrol-1-yl

Scheme 1. Reagents and conditions: (a) R^1-H, NaH (40–100%); (b) NaOH, water, MeOH/dioxane (48–100%); (c) 4-methylpiperidine, EDC, HOBt, or 4-methylpiperidine, HATU, trialkylamine (30–100%); (d) HCl or TFA (73–100%); (e) R^2SO_2Cl, trialkylamine (20–100%).

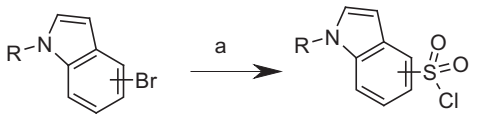

42 a **R** = H; 6-substituted
b **R** = H; 4-substituted
c **R** = Me; 4-substituted
d **R** = Boc; 7-substituted
e **R** = H; 5-substituted
f **R** = Boc; 5-substituted

Scheme 2. Reagents and conditions: (a) NaH (R = H only), -*t*BuLi, saturated SO_2 in THF, then NCS (23–78%).

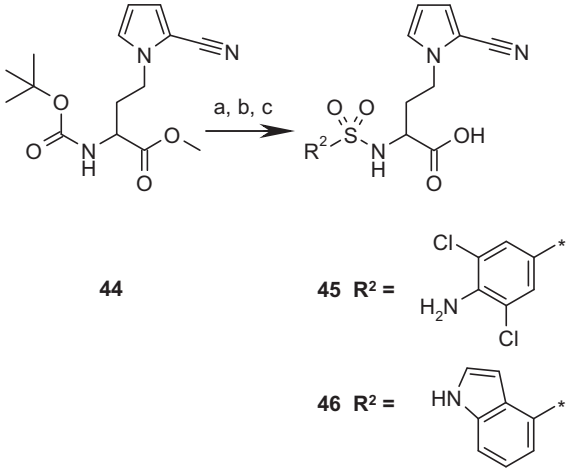

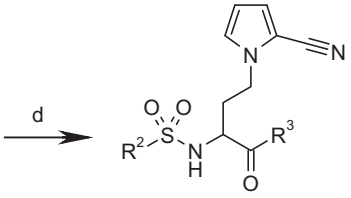

45: **25, 27, 30, 32, 34, 36, 37**

46: **26, 28, 29, 31, 33, 35, 38**

Scheme 3. Reagents and conditions: (a) HCl (66–100%); (b) R^2-SO_2Cl, base (**45**: 67%, **46**: 66%); (c) NaOH; (d) HATU, base, R^3-amine; or EDC, HOBt, R^3-amine (23–51%).

The synthesis of amide analogues is illustrated in Scheme 3. The Boc group of **44** is removed under acidic conditions, and reaction with sulfonyl chlorides followed by saponification delivered **45** and **46**. Amide coupling with HATU or EDC/HOBt then delivered amide analogues **25**–**38**.

We began to find replacements for the nitroimidazole by assessing whether the nitro group was necessary for CCR10 potency (Table 1). While the nitro group improves potency over the unsubstituted imidazole **2**, it can be replaced with either cyano or chloro (cf. **3** and **4** to **1**). By exploring replacements to the imidazole, we also discovered that the imidazole is not ideal. In the absence of a 2-subtituent, a distally disposed aza group (analogous to the imidazole 3-position as with **2**, **5** and **7**) is detrimental to

Table 1
Structure–activity relationships for modifications at R^1

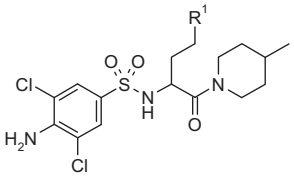

Compound	R^1	Human CCR10 pIC_{50}[a]	Chemotaxis CCL27 pIC_{50}[a]	Murine CCR10 pIC_{50}[a]
1	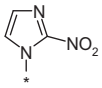	6.2 ± 0.2	7.3 [7.0, 7.5]	<4.7
2		<4.7[b]		
3	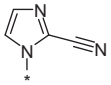	6.3 [6.0, 6.5]		
4		6.3 [6.2, 6.5]	6.6 (n = 1)	<4.7
5		<4.7		
6		5.5 [5.4, 5.5]	5.9 (n = 1)	
7		<4.7		
8		5.8 [5.8, 5.9]	5.9 [5.7, 6.0]	
9		5.4 (n = 1)		
R-**10** *S*-**10**		6.2 [6.2, 6.2] <5.0	6.3 (n = 1) <5.0	5.0 [4.9, 5.0]
11		6.9 [6.8, 7.1]		
12	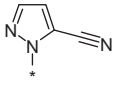	7.2 [7.1, 7.3]		5.5 [5.4, 5.6]
13		6.6 [6.6, 6.7]		
14	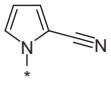	7.7 ± 0.2	7.8 ± 0.3	5.8 ± 0.2

[a] Average ± SD when ⩾3 replicates, a range is shown when 2 replicates.
[b] pIC_{50} from fluorescence imaging assay under the same conditions and in the same CHO-K cell line as the chemiluminescent assay.

potency. Compounds lacking the 3-aza substituent (e.g. **6**, **8**, **9** and **10**) have potency in the range of 0.6–4 μM. As with the imidazole, the presence of a chloro or cyano adjacent to the chain linkage on phenyl (**11**), pyrazole (**12**, **13**), and pyrrole (**14**) improved potencies to levels comparable to or greater than the imidazoles **1**, **3** and **4**.

Please cite this article in press as: Abeywardane, A.; et al. *Bioorg. Med. Chem. Lett.* (2016), http://dx.doi.org/10.1016/j.bmcl.2016.09.047

The enantiomerically pure homophenylalanine analogs *R*-**10** and *S*-**10** demonstrate a strong stereospecificity for CCR10 antagonism that was also observed for the enantiomer pairs of **1** (pIC_{50}'s of 6.3 vs <4.7) and **14** (pIC_{50}'s of 8.1 vs 4.8).

We discovered chlorophenyl **11**, chloropyrazole **13** and cyanopyrrole **14** that effectively bypass the concerns of the nitroimidazole while significantly improving potency over **1**. While modifications in this region did not improve the murine/human selectivity factor, murine potencies improved as the potencies for the human receptor improved.

Similar to R^1, the sulfonamide substituent (R^2) of **1** presented a need to establish SAR, optimize potency, and contend with an undesirable structural feature. In this case, the structural feature is an aniline that could be associated with hepatotoxicity, carcinogenicity, and drug–drug interactions.[18] We prepared >100 diverse sulfonamides with a cyanopyrrole at R^1, but none were more potent than **14**. However, anilines were disproportionately represented among the most potent compounds. While only four examples in the array contained anilines,[19] **14** and three additional anilines were among the ten compounds pIC_{50}'s of ⩾7 (Table 2; **16**, **17**, and **18**; see Fig. S-1 in the Supplementary Material). Moreover, because anilines were among the only polar functional groups tolerated in this region, these same anilines were among the compounds with the highest lipophilic efficiencies (LiPE = LLE = $pIC_{50} - \log D$). Higher LiPE's are associated with improved drug-likeness and a lower potential for off-target activity.[20,21]

In order to capitalize on the apparent potency contribution of the anilines while mitigating their potential liabilities, we hypothesized that indoles would have similar hydrogen-bond donating

Table 2
Structure–activity relationships for modification of the sulfonamide (R^2)

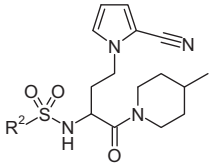

Compound	R^2	Human CCR10 pIC_{50}[a]	Chemotaxis CCL27 pIC_{50}[a]	Murine CCR10 pIC_{50}[a]
14	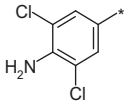	7.7 ± 0.2	7.8 ± 0.3	5.8 ± 0.2
15		5.9 ± 0.2		<4.7 (n = 1)
16	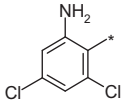	7.4 [7.4, 7.5]		
17	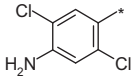	7.2 [7.1, 7.3]		
18	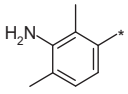	7.0 [6.8, 7.2]	7.1 [7.0, 7.1]	
19	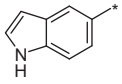	6.7 [6.7, 6.8]	7.9 ± 0.1	
20	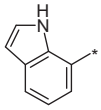	6.6 (n = 1)		5.1 (n = 1)
21	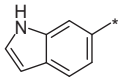	8.1 ± 0.1	7.8 ± 0.1	6.0 ± 0.2
rac-**22** **eut-22** **dis-22**	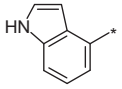	8.7 ± 0.2 9.0 [8.9, 9.1] 5.5 ± 0.1	9.0 ± 0.3	7.2 ± 0.2 7.6 [7.4, 7.9] 4.8 [4.7, 4.8]
23	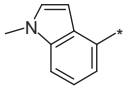	6.9 [6.6, 7.1]		5.2 ± 0.1
24	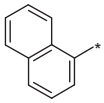	7.3 ± 0.1		

[a] Average ± SD when ⩾3 replicates, a range is shown when 2 replicates.

and electron-donating properties to the anilines without the propensity for bioactivation to reactive species. As there did not appear to be a strongly favored aniline geometry, a variety of indole sulfonamides were prepared (Table 2). Two 5-yl and 7-yl indole analogues (**19** and **20**) are less potent than the most similar anilines. In contrast, **21** and **22** are more potent than the most closely related aniline (**18**). The NH of **22** seems to play a significant role in its potency as the *N*-methyl indole **23** is ~70-fold less potent than *rac*-**22** but is similarly potent to its isostere naphthylenesulfonamide **24**.

The combination of the indole with the cyanopyrrole in **22** substantially improved potency compared to compound **1** and eliminated the risks associated with both the nitroimidazole and the aniline found in **1**. The resolved enantiomers of **22** demonstrate stereospecificity for CCR10 antagonism consistent with the homophenylalanine analogue **10**. While the shift in potency between the human and murine receptors persists, the potency gains achieved in **eut-22** translate to murine receptor antagonism as well, bringing murine potency to a level sufficient for testing in vivo.

New opportunities were not revealed with modification of the methylpiperidine amide. Among the R^3 amide analogues of **14** and **22** we explored, the 4-methylpiperidine remained the most potent. Examples in Table 3 illustrate the general observation that the 4-methyl substituent imparts potency not observed with larger (**27** and **28**) or more polar (**29**) piperidine 4-substituents. The placement of the methyl substituent on the piperidine ring is also important (**30**–**33**). In addition, the piperidine amide is superior to the homologated ring (**34** and **35**) and truncated ring amides (eg. **36**).

We characterized key compounds for further evidence that the functional effects on Ca^{2+} flux and chemotaxis are a consequence of direct interaction with CCR10 (Table 4). Compound **14** competitively and reversibly binds CCR10 with an IC_{50} of 3.4 nM, as detected in an immunochemical binding assays with Fc-CCL27 fusion. These compounds also inhibit the Ca^{2+} flux stimulated from the other known chemokine ligand of CCR10, CCL28/MEC as determined from both fluorescent (FLIPR™) and chemiluminescent readouts. Both **14** and **22** affect CCR10's coupling with G-protein as detected in a GTP-binding assay (GTP-Eu).[22] Compounds **14** and **22** also inhibit CCL27 dependent cAMP production in CCR10 transfected HEK cells. No meaningful binding or activity was observed against 29 GPCR's, including six chemokine receptors (Table 5 in the Supplementary Material). The consistency of the various functional readouts (Ca^{2+} flux, cAMP production, GTP binding, and chemotaxis) across three cell backgrounds (CHO-K, HEK, and

Table 3
Structure–activity relationships for modification of the amide (R^3)

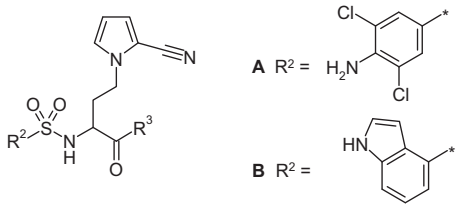

R^3	R^2 = A Compound	Human CCR10 pIC_{50}[a]	R^2 = B Compound	Human CCR10 pIC_{50}[a]
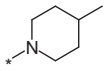	**14**	7.7 ± 0.2	*rac*-**22**	8.7 ± 0.2
	**25**	6.8 [6.6, 6.9]	**26**	8.0 [8.0, 8.0]
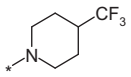	**27**	6.4 [6.3, 6.5]	**28**	8.0 ± 0.2
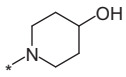			**29**	6.9 [6.9, 7.0]
	**30**	6.1 [6.0, 6.1]	**31**	7.7 [7.7, 7.7]
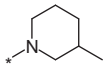	**32**	6.2 [6.1, 6.3]	**33**	7.2 [7.1, 7.2]
	**34**	6.6 [6.6, 6.6]	**35**	7.6 [7.5, 7.7]
	**36**	<5.0 (n = 1)		
	**37**	<5.0 (n = 3)	**38**	5.4 ± 0.1

[a] Average ± SD when ⩾3 replicates, a range is shown when 2 replicates.

Table 4
Summary of CCR10 antagonism data for select compounds

Assay	Cell line	Agonist/probe	Compound		
			1	**14**	**rac-22**
Competition binding pIC_{50}	HEK membrane prep	hCCL27-Fc		8.5	
FLIPR Ca^{2+} flux pIC_{50}	CHO-K (Aequorin, Gαq)	hCCL27	6.6 ± 0.3	8.7 ± 0.2	9.4 ± 0.2
FLIPR Ca^{2+} flux pIC_{50}	CHO-K (Aequorin, Gαq)	hCCL28	6.1 ± 0.1	7.9 ± 0.3	8.9 ± 0.2
Aequorin Ca^{2+} flux pIC_{50}	CHO-K (Aequorin, Gαq)	hCCL27	6.2 ± 0.2	7.7 ± 0.2	8.7 ± 0.2
Aequorin Ca^{2+} flux pIC_{50}	CHO-K (Aequorin, Gαq)	hCCL28	6.1 ± 0.1	7.9 ± 0.1	9.0 [8.9, 9.1]
cAMP pIC_{50}	HEK	hCCL27		6.8	7.6
GTP-Eu pIC_{50}	HEK membrane prep	hCCL27		7.7	8.0
Chemotaxis pIC_{50}	Ba/F3	hCCL27	7.3 [7.1, 7.4]	7.9 ± 0.3	9.0 ± 0.3

pIC_{50}s are average ± SD when ⩾3 replicates, a range is shown when 2 replicates, otherwise data from a single test occasion.

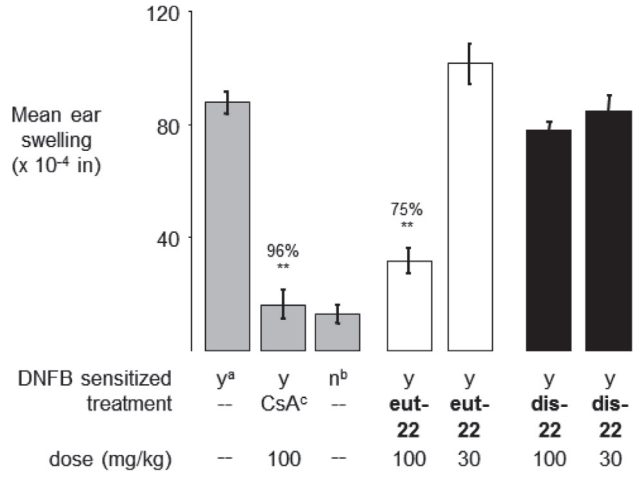

Figure 2. eut-22 but not **dis-22** is efficacious in the DNFB model of murine contact hypersensitivity when dosed at 100 mg/kg ip bid**.** Inhibition of the DNFB stimulated inflammatory response in sensitized Balb-C mice. The readout is ear swelling 24 h after stimulation with DNFB solution. [a]Vehicle control. [b]Background. [c]CsA: cyclosporine A**ρ < 0.05.

Ba/F3), along with the observed specificity of these compounds for CCR10 all support these compounds' activity proceeding through direct interaction with CCR10.

The murine cellular potency and apparent specificity of **22** qualified it as a suitable tool to test the impact of CCR10 antagonism on dermal inflammation. Therefore, **eut-22** was investigated for efficacy against DNFB (2,4-dinitrofluorobenzene) murine contact hypersensitivity (Fig. 2), with **dis-22** serving as a structurally related negative control. The model captures a predominantly T-cell dependent inflammatory response of sensitized mice to topical DNFB challenge on the ear.[23] Due to high clearance of **22** in mice (murine liver microsome $t_{1/2}$ <3 min; >88% Qh), a 100 mg/kg dose delivered intraperitoneally at 0 and 8 h was required to maintain plasma exposure near or above the murine IC_{50} of **eut-22** over the majority of the experiment.[24] Nonetheless, **eut-22** exhibited a dose-dependent anti-inflammatory response against DNFB stimulated ear swelling in sensitized mice. While the eutomer **eut-22** showed efficacy, the distomer **dis-22** demonstrated no activity, consistent with the stereospecificity of CCR10 antagonism. The level of efficacy observed for **eut-22** was similar to that observed with anti-CCL27 antibody in the same model (60–85%).[6]

We report the first small molecule antagonists of CCR10.[25,26] The initial hit from screening, a 690 nM antagonist of CCR10 dependent Ca^{2+} flux, contained both a nitroimidazole and an aniline. Optimization delivered **eut-22** that is not only 300 times more potent a CCR10 antagonist than the initial hit, but eliminated potential toxicity, mutagenicity, and drug–drug-interaction liabilities that can be associated with nitroaryls and anilines. Compound **eut-22** is highly selective for CCR10 over other GPCR's, including a number of other chemokine receptors. Finally, **eut-22** is efficacious in a murine model of DNFB contact hypersensitivity. The efficacy of this compound provides further evidence for the role of CCR10 in dermatological inflammatory conditions. These small molecule inhibitors may also be valuable in interrogating the role of CCR10 in mucosal inflammation (e.g. asthma)[26] and cancer.[5]

Supplementary data

Supplementary data associated with this article can be found, in the online version, at http://dx.doi.org/10.1016/j.bmcl.2016.09.047.

References and notes

1. Butcher, E. C.; Picker, L. J. *Science* **1996**, *272*, 60.
2. Kupper, T. S.; Fuhlbrigge, R. C. *Nat. Rev. Immunol.* **2004**, *4*, 211.
3. Williams, I. R. *Immunol. Res.* **2004**, *29*, 283.
4. Fu, Y.; Yang, J.; Xiong, N. *J. Immunol.* **2016**, *196*, 4859.
5. Xiong, N.; Fu, Y.; Hu, S.; Xia, M.; Yang, J. *Protein Cell* **2012**, *3*, 571.
6. Homey, B.; Alenius, H.; Muller, A.; Soto, H.; Bowman, E. P.; Yuan, W.; McEvoy, L.; Lauerma, A. I.; Assmann, T.; Bunemann, E.; Lehto, M.; Wolff, H.; Yen, D.; Marxhausen, H.; To, W.; Sedgwick, J.; Ruzicka, T.; Lehmann, P.; Zlotnik, A. *Nat. Med.* **2002**, *8*, 157.
7. Campanati, A.; Goteri, G.; Simonetti, O.; Ganzetti, G.; Giuliodori, K.; Stramazzotti, D.; Morichetti, D.; Bernardini, M. L.; Mannello, B.; Fabris, G.; Offidani, A. *Br. J. Dermatol.* **2007**, *157*, 1155.
8. Hijnen, D.; De Bruin-Weller, M.; Oosting, B.; Lebre, C.; De Jong, E.; Bruijnzeel-Koomen, C.; Knol, E. *J. Allerg. Clin. Immunol.* **2004**, *113*, 334.
9. Fujimoto, S.; Uratsuji, H.; Saeki, H.; Kagami, S.; Tsunemi, Y.; Komine, M.; Tamaki, K. *Cytokine* **2008**, *44*, 172.
10. Mirshahpanah, P.; Li, Y. Y.; Burkhardt, N.; Asadullah, K.; Zollner, T. M. *Exp. Dermatol.* **2008**, *17*, 30.
11. Reiss, Y.; Proudfoot, A. E.; Power, C. A.; Campbell, J. J.; Butcher, E. C. *J. Exp. Med.* **2001**, *194*, 1541.
12. Soler, D.; Humphreys, T. L.; Spinola, S. M.; Campbell, J. J. *Blood* **2003**, *101*, 1677.
13. Le, P. E.; Hisada, S.; Mizuguchi, Y.; Dupriez, V. J.; Burgeon, E.; Detheux, M. *J. Biomol. Screen.* **2002**, *7*, 57.
14. Boelsterli, U. A.; Ho, H. K.; Zhou, S.; Leow, K. Y. *Curr. Drug Metab.* **2006**, *7*, 715.
15. Abeywardane,A.; Cogan, D.; Choi, Y.; Gao, D.A.; Goldberg, D.R.; Heim-Riether, A.; Miller, C.; Ramsden, P.D.; Smith Keenan, L.L.; Snow, R.J.; Yang, Y. U.S. Patent 8,586,748, 2011.
16. Thompson, M. J.; Mekhalfia, A.; Hornby, D. P.; Blackburn, G. M. *J. Org. Chem.* **1999**, *64*, 7467.
17. Heim-Riether, A. *Synthesis* **2008**, 883.
18. Kalgutkar, A. S.; Dalvie, D. K.; O'Donnell, J. P.; Taylor, T. J.; Sahakian, D. C. *Curr. Drug Metab.* **2002**, *3*, 379.
19. Compounds were prepared from sulfonyl chlorides with unreactive anilines. Due to aniline reactivity toward the sulfonyl chlorides, less substituted analogues were not prepared.
20. Shultz, M. D. *Bioorg. Med. Chem. Lett.* **2013**, *23*, 5980.
21. Ryckmans, T.; Edwards, M. P.; Horne, V. A.; Correia, A. M.; Owen, D. R.; Thompson, L. R.; Tran, I.; Tutt, M. F.; Young, T. *Bioorg. Med. Chem. Lett.* **2009**, *19*, 4406.
22. Frang, H.; Mukkala, V. M.; Syysto, R.; Ollikka, P.; Hurskainen, P.; Scheinin, M.; Hemmila, I. *Assay Drug Dev. Technol.* **2003**, *1*, 275.
23. Saint-Mezard, P.; Berard, F.; Dubois, B.; Kaiserlian, D.; Nicolas, J. F. *Eur. J. Dermatol.* **2004**, *14*, 131.

24. Satellite exposures of compound in 30% cremophore dosed in Balb-C mice: **eut-22**, 100 mg/kg ip, 1 h: 7.6 ± 4.5 μM, 7 h: 0.2 ± 0.2 μM; 30 mg/kg ip, 1 h: 3.7 ± 0.4 μM, 7 h: not detected. **dis-22**, 100 mg/kg ip, 1 h: 18 ± 2 μM; 7 h: not detected; 30 mg/kg ip, 1 h: 3.2 ± 0.8 μM, 7 h: not detected; 99% plasma protein binding for both compounds.
25. Jung, F.; Gombert, F.O.; Obrecht, D.; Bisang, C.; Bayly, C.I.; Bayly, C.I.; Barthélémy, S.; Lederer, A.; Chevalier, E. U.S. Patent 8,754,038, 2014.
26. Daubeuf, F.; Jung, F.; Douglas, G. J.; Chevalier, E.; Frossard, N. *Respir. Res.* **2015**, *16*, 1.